

# Mechanical energy losses due to the movement of dislocations in molybdenum at high temperatures ( $0.3T_m$ )

G.I. Zelada-Lambri<sup>a</sup>, O.A. Lambri<sup>a,b,\*,1</sup>, J.A. García<sup>c</sup>

<sup>a</sup> *Facultad de Ciencias Exactas, Ingeniería y Agrimensura, Universidad Nacional de Rosario, Laboratorio de Materiales, Escuela de Ingeniería Eléctrica, Avda. Pellegrini 250, (2000) Rosario, Argentina*

<sup>b</sup> *Instituto de Física Rosario, Argentina*

<sup>c</sup> *Departamento de Física Aplicada II, Facultad de Ciencias, Universidad del País Vasco, Apdo. 644, 48080 Bilbao, País Vasco, Spain*

Received 8 August 2005; accepted 7 February 2006

## Abstract

Damping measurements were performed, at around 1 Hz, in high purity single crystalline molybdenum from room temperature up to 1273 K. The results showed that the intensity of the damping peak at around 840–1050 K depended on the degree of plastic deformation at room temperature. Moreover the peak temperature and activation energy of this relaxation increased with the temperature of the previous annealing of the sample, and was independent of the crystal orientation. In addition, once the damping peak appeared after annealing, the damping values were independent of the amplitude of oscillation. Possible physical mechanisms involving dislocations interaction are discussed.

© 2006 Elsevier B.V. All rights reserved.

PACS: 61.50.-f; 61.72.Lk; 61.72.jj; 62.40.+i

## 1. Introduction

Molybdenum, a group VI of transition metal has a high melting point, a high specific heat, and good corrosion and creep resistance and strength at high temperatures. These qualities make molybdenum attractive for the use in the nuclear industry. In fact molybdenum and its alloys are used, for example, in

nuclear reactor vessels and other reactor components, detectors in control systems of Tokamak devices and recently they have attracted interest as components for the development of space nuclear reactor power systems [1–3].

Mechanical spectroscopy, referred also to as internal friction method is a non destructive technique and is a fundamental tool for studying the movement of dislocations and their interaction with point defects. The internal friction of molybdenum exhibits three main peaks, namely,  $\alpha$ ,  $\beta$  and  $\gamma$ , in the 50–450 K temperature range at a frequency of measurement of 1 Hz. Dislocation mechanisms associated with the above damping peaks have been proposed. For recent reviews see Benoit [4] and Seeger

\* Corresponding author. Address: Facultad de Ciencias Exactas, Ingeniería y Agrimensura, Universidad Nacional de Rosario, Laboratorio de Materiales, Escuela de Ingeniería Eléctrica, Avda. Pellegrini 250, (2000) Rosario, Argentina. Tel.: +54 341 4802649; fax: +54 341 4821772/4802654.

E-mail address: [olambri@fceia.unr.edu.ar](mailto:olambri@fceia.unr.edu.ar) (O.A. Lambri).

<sup>1</sup> Member of the CONICET's Research Staff.

[5]. In previous works [6,7] we also studied the internal friction of molybdenum single crystals from liquid nitrogen temperature to 450 K. The differences between the annealing curves for the annealed and the cold-worked samples and the changes in irradiation have successively been explained using a point defect dragging model. A  $\beta$  peak at 150 K in heavily cold-worked samples and a direct and an inverse-modulus defect seen at the same temperature were all attributed to the dragging of point defects trapped at kinks on the dislocations.

Due to the lack of information in the literature concerning the internal friction of molybdenum for temperature higher than 600 K, we extended the temperature range of study to 1300 K [8]. We found an intense relaxation peak in the 840–1040 K region for single crystalline samples previously deformed at room temperature and annealed at temperatures above that for vacancy diffusion. The peak showed a hysteresis between the warming – cooling runs, but was not affected by a bias stress. The peak temperature, intensity and activation energy differed in the two samples measured which were of different orientation ( $\langle 110 \rangle$  and  $\langle 149 \rangle$ ).

In the present work we have studied the following features: The dependence of the peak height by varying the pre-strain at room temperature. The dependence of the activation energy both on temperature and crystal orientation. The appearance of amplitude dependent damping effects in the whole temperature range of the damping peak for different thermomechanical histories.

## 2. Experimental

The single crystals used in this work were prepared from zone refined single-crystal rods of molybdenum in A.E.R.E., Harwell. The residual resistivity, RR, of the samples was about 8000, the main residual impurity, being tungsten. RR is calculated from the ratio between the electrical resistivity value measured at room temperature and the value of the electrical resistivity measured at liquid helium temperatures. Samples with the  $\langle 110 \rangle$  and  $\langle 149 \rangle$  crystallographic tensile axis were used to favour deformation by multiple and single slip; respectively. The samples were sheets of 20 mm length, 0.1 mm thickness and 2 mm width. The samples were annealed and then deformed in extension at a constant speed of 0.03 cm/min, followed by torsion at room temperature. The status of the samples used is shown in Table 1.

Table 1  
Sample descriptions

Sample type	Orientation	Elongation (%)	Torsion (%)	Quantity of samples tested
I	$\langle 110 \rangle$	5	1	1
II	$\langle 110 \rangle$	3	1	2 (a and b samples)
III	$\langle 149 \rangle$	5	1	2 (a and b samples)

Single crystals, after plastic deformation and damping tests, were checked by means of Laue photographs and metallographical study. Laue photographs were performed in a Leybold 554-61 GmbH equipment with copper radiation. The usual etching for revealing grain boundaries in molybdenum was employed, i. e. a mix of potassium hydroxide 10 g plus water 100 ml and potassium ferricyanide 10 g plus water 100 ml [9]. Other etchants were also used such as: concentrated and diluted sulphuric acid and ammonia plus hydrogen peroxide plus water [9].

Laue and light microscopy studies indicated that the single crystalline state was not changed by the plastic deformation or annealing to the work temperatures.

Damping,  $Q^{-1}$  (or internal friction), and natural frequency were measured in an inverted torsion pendulum, under a vacuum of about  $10^{-5}$  Pa. The equipment can also apply a bias stress or ‘in situ’ deformation. The maximum strain on the surface of the sample was  $5 \times 10^{-5}$ . The measurement frequency was around 1 Hz except in the determination of the frequency dependence of the peak temperature. The heating and cooling rates employed in the test were of 1 K/min. There was no hold time once the maximum temperature had been achieved.

During the run-up in temperature  $Q^{-1}$  was calculated from the slope of the straight line which results from the least squares fitting of the natural logarithm of all the decaying amplitudes versus time, such that

$$\ln(A_n) = \ln(A_0) - \pi Q^{-1}n, \quad (1)$$

where  $A_n$  is the area of the  $n$ th decaying oscillation,  $A_0$  is the initial area of the starting decaying oscillation and  $n$  is the period number. For all these measurements the same initial and end values of the decaying amplitudes were used eliminating some possible distortion due to amplitude dependent damping effects [10].

The longest time employed for recording the decay during the heating runs was shorter than 60 s. In fact, in order to hold the ratio between  $A_n$  and  $A_0$  at  $Q^{-1}$  values of about 0.01; the recording time was about 10 s. Consequently each point plotted in Figs. 1 and 2 have an accuracy in temperature better than 1 K.

Amplitude dependent damping (ADD) effects were very small and the corrections to intrinsic values of the measured damping can be neglected.

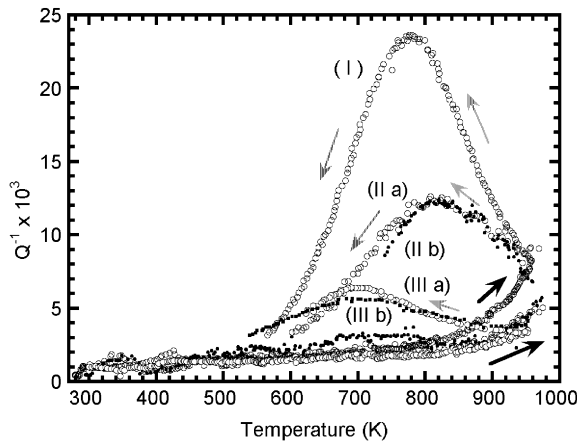


Fig. 1. Damping spectra measured during the first warm ups and subsequent cooling after room temperature deformation for different samples. Labels in the curves indicate the sample type as specified in Table 1. Full and broken arrows indicate the warming and cooling runs, respectively.

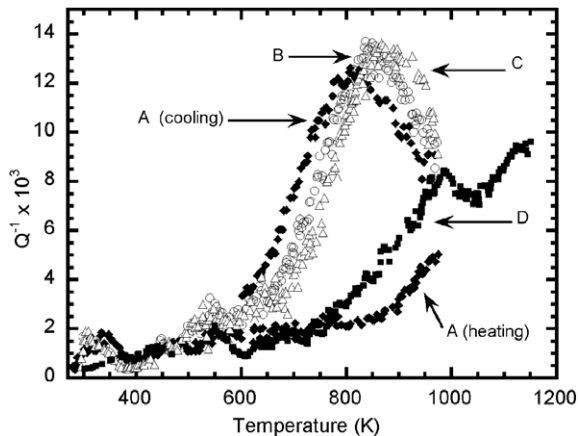


Fig. 2. Damping spectra measured for a sample of type II during different heating runs. (A) After deformation at room temperature. (B) and (C) are the subsequent runs up to 970 K. (D) Run correspond to a heating after an annealing to 1200 K.

However, the analysis of the ADD was developed in the present work as it brings out very useful information on the nature of the pinning.

Damping as a function of the maximum strain amplitude on the sample,  $\varepsilon_0$ , was calculated from Eq. (2) [10]

$$Q^{-1}(\varepsilon_0) = -\frac{1}{\pi} \frac{d(\ln(A_n))}{dn}. \quad (2)$$

The decay of the oscillations were studied at constant temperature ( $T \pm 0.5^\circ$ ). Polynomials were fit to the curve of the decaying areas of the torsional vibrations as a function of the period number by means of Chi-square fitting. Subsequently, Eq. (2) was applied. Polynomials of order higher than 1 indicate that  $Q^{-1}$  is a function of  $\varepsilon_0$ , due to the appearance of ADD effects. This procedure allows damping as a function of the maximum strain ( $\varepsilon_0$ ) to be obtained from free decaying oscillations [10–12]. The order of fitted polynomials was smaller than 3.

### 3. Results

#### 3.1. Dependence of the peak height and peak temperature on orientation, the degree of plastic deformation and annealing temperature

Fig. 1 shows the damping spectra measured in the different sample types detailed in Table 1. During the first heating, after the room temperature deformation, the samples showed an increasing background with temperature. Nevertheless, on cooling a well developed internal friction peak was present. The peak height and temperature are reproducible for samples of the same type but are strongly dependent both on the orientation and on the plastic deformation degree.

The behaviour of the peak for type I and III samples on consecutive warm ups has been previously reported [8]. Similar behaviour has been found in the type II samples and is shown in Fig. 2. The peak moves to a slightly higher temperature and increases in intensity on consecutive heating to 973 K, but then stabilised at a peak temperature of about 840 K, (runs B and C). When the maximum annealing temperature is increased to 1250 K, the peak temperature changes to 970 K (see D curve) and the intensity of the peak is decreased. Further runs to 1250 K decrease more the intensity of the peak.

For all the samples in Table 1 the peak, after the background subtraction, moves to a slightly higher temperature and increases in intensity on consecutive runs-up to 973 K (973 K was the maximum annealing temperature reached during the first series of runs-up). After three heating runs up to 973 K the peak stabilised.

When the maximum annealing temperature is increased to temperatures close to 1250 K for the I and III samples, the peak temperature changes to higher temperatures. This temperature change is accompanied by a decrease in the intensity of the peak. In addition, further runs to 1250 K reduce the intensity of the peak and it disappears if the sample keeps vibrating for long time at 1250 K.

For the II samples the maximum temperature of the thermal cycles was increased in smaller steps than for I and III samples. In fact, the shifting in the peak temperature and the decrease in its intensity, varied progressively as the temperature in the test increased.

In order to summarise the behaviour of the peak in all the samples during the successive thermal cycles, the peak temperature and the peak height as a function of the maximum temperature of the previous anneal are plotted in Figs. 3 and 4, respectively. Plotted values were obtained after background subtraction and after the stabilisation of the damping spectra.

Background subtraction was performed using cubic polynomials by means of Peak Fit software [13]. The largest error-bandwidth in the peak tem-

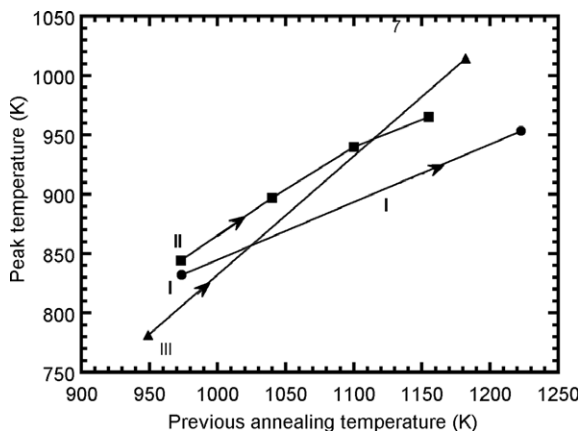


Fig. 3. Peak temperature as a function of the maximum temperature reached in the previous test. Circles: type I sample, squares: II sample, triangles: III sample.

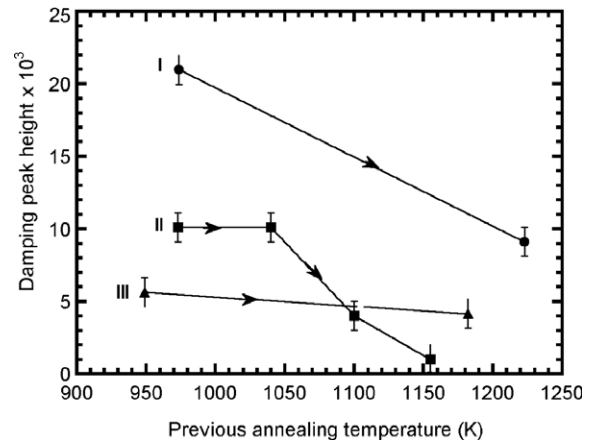


Fig. 4. Damping peak height as a function of the maximum temperature reached in the previous damping test. Labels and symbols indicate as in Fig. 3.

perature,  $T_p$ , was smaller than 3 K. The largest variation in  $T_p$  obtained from different polynomials of order 2 and 3 for fitting the background was considered as the error-bandwidth. Consequently the error-bandwidths are smaller than the size of the symbols plotted in Fig. 3.

Increasing the temperature of the thermal cycles above 973 K, after the three heating performed up to 973 K, the peak was stable in its new state (peak height and peak temperature), i.e. the peak did not change by successive run-ups in temperature up to the same maximum temperature. However, as it was previously mentioned the peak disappears after a long time of vibration at 1250 K, but this is not the case for data plotted in Figs. 3 and 4.

We indicate the smallest temperature for thermal cycles as 973 K. However for samples of type III, some cycles were performed up to 950 K or 960 K, but this difference is not significant and does not detract from the subsequent analysis.

### 3.2. Activation energy as a function of the peak temperature

In order to calculate the activation energy of a peak, the frequency dependence of the peak temperature was measured once the peak had stabilised after thermal cycling. Measurements were made at natural frequencies (at room temperature) of around 0.2 Hz, 0.7 Hz and 2 Hz.

Fig. 5 shows the Arrhenius plots for the samples detailed in Table 2. The lines join points from a

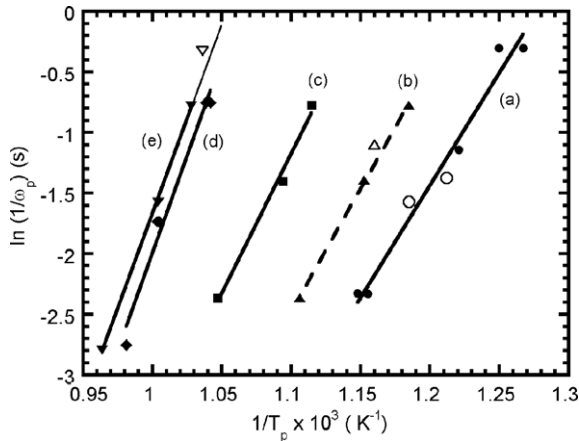


Fig. 5. Arrhenius plot related to the samples specified in Table 2.

Table 2

Details of the samples used in the determination of activation energy as a function of peak temperature and the symbol terminology in Fig. 5

Plot	Symbol/ Sample type	$T_p$ (K)/ $f_p$ (Hz)	$\Delta(1/T_p) \times 10^3$ ( $K^{-1}$ )	$H$ (eV)
a	●/I ○/II (b) ○/II (a)	825/0.63 844/0.77	4.4	$1.6 \pm 0.1$
b	▲/II △/I	862/0.5	4.0	$1.80 \pm 0.03$
c	■/II		4.0	$2.00 \pm 0.07$
d	◆/I		3.0	$2.8 \pm 0.1$
e	▼/III ▽/II	965/0.22	3.0	$2.70 \pm 0.04$

$T_p$  and  $f_p$  are the temperature and the frequency evaluated at the peak.  $\Delta(1/T_p)$  is the error-bandwidth corresponding to  $1/T_p$ .

given sample. The open symbols represent data points from other samples. Data represented by empty triangles were obtained from a regenerated peak, after its disappearance by long time annealing at 1250 K, due to plastic redeformation of the I sample in torsion in situ in the pendulum. Since they fit on lines from a different sample type, it suggests that the activation energy only depends on the temperature at which the peak occurs.

The errors in  $T_p$  lead to error-bandwidths in the reciprocal temperature,  $\Delta(1/T_p)$ , slightly smaller than the size of the symbols. The largest bandwidths employed in the fitting process are written in Table 2 for each kind of sample. In contrast, the error in the frequency can be neglected.

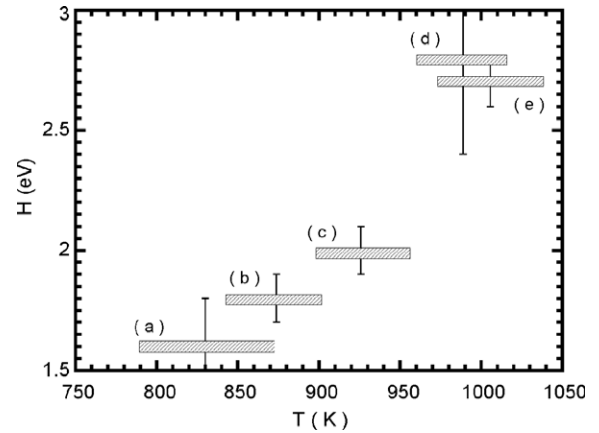


Fig. 6. Activation energy values,  $H$ , as a function of the temperature interval employed for their calculus.

The results show that the activation energy changes with the temperature of the peak. We have assumed for calculating the activation energy by means of the Arrhenius formalism, that the activation energy of the relaxation is constant within the temperature range covered by the frequency change. Therefore, the calculated value refers to an average value integrated over about 70 K.

The error written for  $H$  in Table 2 were determined considering the error margins of the fit curve, i.e. the slopes of the maximum and minimum straight-lines.

Despite of the size of the error band-width for  $H$ , its dependence on temperature is clear. In fact, Fig. 6 shows  $H$  against the temperature interval employed for its calculus.

### 3.3. Amplitude dependent damping effects

ADD is only seen in the first warming curve after the deformation process. The strength of the effect is characterised by the parameter  $S$  defined by  $S = \Delta Q^{-1}/\Delta \epsilon_0$  i.e. the slope of the curve of damping as a function of strain.

Fig. 7 shows some curves of the whole group of the damping against maximum strain amplitude measured at different (constant) temperatures for the first warm up of type I samples.

Fig. 8 shows the  $S$  parameter for the three types of samples. The results for the second, third and fourth warm up are included to show that no ADD effects occur once the damping peak has developed. Moreover the  $S$  values in the first warm up are largest for the type I sample which developed the largest damping peak.

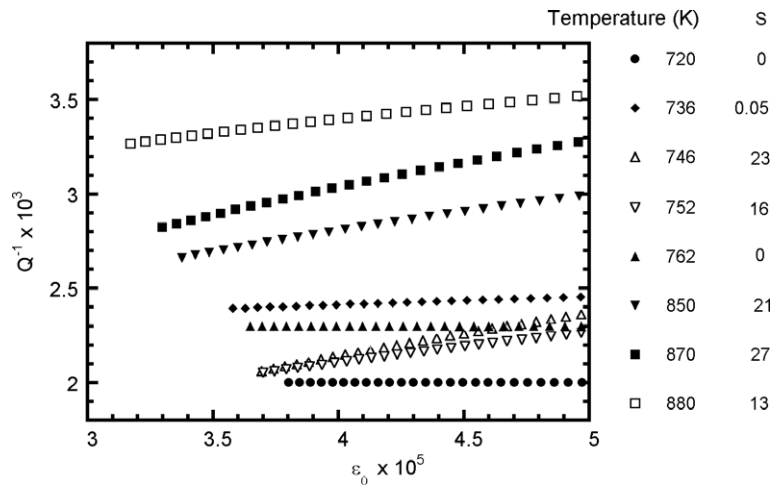


Fig. 7. Damping as a function of the maximum amplitude strain,  $\epsilon_0$ , on a type I sample measured at several constant temperatures during the first run-up in temperature after plastic deformation at room temperature. The temperatures are shown at the side.

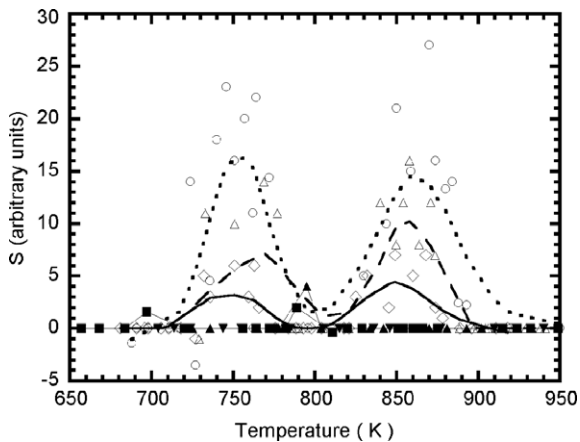


Fig. 8.  $S$  as a function of temperature for various type samples and heating runs. Circles, type I; triangles, type II; diamond, type III. The open symbols show the results from the first heating after the room temperature deformation and the full symbols show the results from the second, third and fourth heating runs.

#### 4. Discussion

Previous work on the internal friction of deformed molybdenum at high temperatures [8] showed that the observed peak in the damping is closely related to the interaction of vacancies and dislocations introduced by deformation. Samples with  $\langle 149 \rangle$  and  $\langle 110 \rangle$  tensile axes were used to favour single and multiple slip, respectively.

The dislocation structure of deformed molybdenum has been studied by transmission electron microscopy (TEM) in other work [14–18]. Samples deformed at room temperature in the deformation

range used in the present work show long screw dislocations with a high density of jogs but few edge dislocations. However, dislocation fragments with Burgers vectors  $a\langle 100 \rangle$  and a high density of prismatic loops were present. They are effective obstacles to glide and play an important role in dislocation tangling.

The TEM observations strongly suggest that screw dislocations are involved in the damping peak observed in the present work.

In a recent review of the relaxations seen in molybdenum at lower temperatures, Seeger [5] suggests that diffusion of kinks and kink pair formation on screw dislocations are responsible for the  $\alpha$  and  $\gamma$  relaxations respectively. It was previously shown [8] by application of a bias-stress during measurement that cross-slip of screw dislocations could not be involved in the mechanism. However the high density of jogs observed by TEM suggests that dragging of sessile jogs by the mobile screw dislocations assisted by vacancy diffusion and/or generation could give rise to the damping peak. The observed intensity of the peaks in the different type samples (Fig. 1) are consistent with a low dislocation and jog density in single slip (the  $\langle 149 \rangle$  type III samples). Moreover increasing the strain in the  $\langle 110 \rangle$  samples would increase the density of dislocations and jogs and hence the peak height (type I is longer than type II).

Vacancies are produced during deformation by the non-conservative movement of jogs. The presence of ADD effects during the first warm-up suggests that the vacancies are distributed on the

dislocation lines and that ADD arises from the hysteretic break away of the dislocations during vibration. The damping peak only develops after the sample has been heated to the temperature range where the vacancy is mobile. The vacancies may leave the dislocations, coalesce on the line to form stronger pinning points or may interact with the jogs.

The vibration of the dislocation may drag the vacancy-jog complex and cause the damping peak or the vacancy complex may move along the line. At temperatures up to 970 K the peak stabilises after a few warm ups, showing that only minor rearrangement of the vacancies occurs. However on heating to higher temperatures the peak is reduced in height and occurs at a higher temperature. If a further movement of the vacancies can occur above 970 K there may be progressively less complexes with a greater pinning strength which would account for the observed peak behaviour. Finally, the complex might become immobile and the peak would disappear as seen for prolonged vibration.

The present results show that the change in the value of activation energy reported in the previous work [8] is not related to the sample orientation, but to the peak temperature and thermal treatment of the sample.

Calculations of the activation energies for diffusion along the dislocation have been reviewed in Ref. [19]. For molybdenum reported values for the migration energy  $H_{vm}$  are between 1.35 eV and 1.60 eV [20–22]. The experimental value of 1.6 eV found for the peak at 800 K shows that vacancy motion on the line could be the origin of the peak. The migration energy for a vacancy complex would be higher and move the peak to higher temperatures as observed. It is not possible to say whether the peak arises from the oscillation of vacancy complexes along the line or from the dragging of the complex with the dislocation line without break away.

## 5. Conclusions

From the present work the following characteristics of the relaxation phenomena at high temperatures in Molybdenum have been established:

- (a) The intensity of the damping peak at around 800–1050 K depends on the degree of plastic deformation at room temperature.

- (b) The activation energy and peak temperature of this relaxation increase with the prior annealing temperature of the sample.
- (c) The activation energy is independent of the crystal orientation.
- (d) Once the damping peak appeared after annealing, the damping values were independent of the amplitude of oscillation. In contrast, amplitude dependent effects appeared during the first warming.

## Acknowledgements

We acknowledge to Professor J.N. Lomer for stimulating discussions and for English revision and to R.J. Tinivella and R.E. Bolmaro for X-ray facilities. This work was partially supported by the Collaboration Agreement between the Universidad del País Vasco and the Universidad Nacional de Rosario Res. CS.788/88-1792/2003 and UPV224. 310-14553/02, the CONICET-PEI No. 6206, the PID-UNR 2003–2004, 2005–2007 and the EIE.

## References

- [1] M.S. El-Genk, J.M. Tournier, *J. Nucl. Mater.* 340 (2005) 93.
- [2] B.V. Cockeram, J.L. Hollembeck, L.L. Snead, *J. Nucl. Mater.* 324 (2004) 77.
- [3] A.A. Ivanov, M.V. Kollegov, V.V. Kolmogorov, E.A. Kuper, A.S. Medveko, A.N. Shukaev, in: 8th International Conference on Accelerator and Large Experimental Physics Control Systems, San José, California, TUAP017, 2001.
- [4] W. Benoit, in: R. Schaller, G. Fantozzi, G. Gremaud (Eds.), *Mechanical Spectroscopy 2001*, Trans. Tech. Publications, Uetikon-Zuerich, Switzerland, 2001, p. 141.
- [5] A. Seeger, *Philos. Mag. Lett.* 82 (2003) 107.
- [6] M.A. Abdergadir, J.A. García, Jenifer Lomer, *Philos. Mag.* (a) 53 (6) (1986) 755.
- [7] J.A. Garcia, Jenifer Lomer, C.R.A. Sutton, W.G. Wood, *Philos. Mag.* (a) 59 (1989) 105.
- [8] O.A. Lambri, G.I. Zelada-Lambri, L.M. Salvatierra, J.A. García, J.N. Lomer, *Mater. Sci. Eng. A* 370 (2004) 222.
- [9] E.A. Brandes, G.B. Brook (Eds.), *Smithells Metals Reference Book*, Butterworth Heinemann, Oxford, 1999, p. 10.
- [10] O.A. Lambri, A review on the problem of measuring non-linear damping and the obtainment of intrinsic damping, in: Martinez-Mardones, Walgraef, Wörner (Eds.), *Materials Instabilities*, 2000, p. 249.
- [11] B.J. Molinas, O.A. Lambri, M. Weller, *J. Alloys Compd.* 211&212 (1994) 181.
- [12] G.I. Zelada-Lambri, O.A. Lambri, G.H. Rubiolo, *J. Nucl. Mater.* 273 (1999) 248.
- [13] *Peak Fit*, V. 4, Jandel Scientific Software, Germany, 1995.
- [14] D. Vesely, *Philos. Mag.* 27 (1972) 603.
- [15] A. Luft, L. Kaun, *Phys. Stat. Sol.* 37 (1970) 781.

- [16] V. Kopetskii, A.I. Pashkansii, *Phys. Stat. Sol. (a)* 21 (1974) 741.
- [17] A. Luft, L. Kaun, *Phys. Stat. Sol.* 18 (1973) 109.
- [18] D. Vesely, *Phys. Stat. Sol.* 29 (1968) 675.
- [19] M.L. Nó, in: R. Schaller, G. Fantozzi, G. Gremaud (Eds.), *Mechanical Spectroscopy 2001*, Trans. Tech. Publications, Switzerland, 2001, p. 247.
- [20] M. Suezawa, H. Kimura, *Philos. Mag.* 28 (1973) 901.
- [21] I.A. Schwirlich, H. Schultz, *Phil. Mag. A* 42 (1980) 601.
- [22] R. Ziegler, H.E. Schaefer, in: *International Conference on Vacancy and Interstitials in Metals and Alloys*, Berlin, September 1986.